Transactions of the Materials Research Society of Japan 25 [1] 185-188 (2000)

Structural and Dielectric Properties of Intergrowth $Bi_4Ti_3O_{12}-SrBi_4Ti_4O_{15}$ Ceramics

Yuji Noguchi, Masaru Miyayama* and Tetsuichi Kudo

Department of Applied Chemistry, School of Engineering, The University of Tokyo,
7-3-1 Hongo, Bunkyo-ku, Tokyo 113-8656, Japan.
*Institute of Industrial Science, The University of Tokyo,
7-22-1, Roppongi, Minato-ku, Tokyo 106-8558, Japan.
Fax : 81-3-3818-0284, e-mail : ynoguchi@imat.chem.t.u-tokyo.ac.jp

Key words : bismuth layer-structured ferroelectrics, Currie temperature, Rietveld analysis, intergrowth structure.

ABSTRACT

The crystal structure of intergrowth $Bi_4Ti_3O_{12}-SrBi_4Ti_4O_{15}$ (BIT-SBTi) was analyzed by the Rietveld method and the phase transition was evaluated by dielectric and differential thermal analysis (DAT) measurements. The Rietveld analysis showed the direct evidence of the continuity of the regular intergrowth structure spread through the crystal. The ferroelectric phase transition of the intergrowth BIT-SBTi was found to occur at the middle of the Curie temperatures of constituent $Bi_4Ti_3O_{12}$ and $SrBi_4Ti_4O_{15}$ and to be of the first-order type.

1. INTRODUCTION

When a voltage is applied to ferroelectrics and then switched off, a certain amount of macroscopic polarization is preserved in the material. For its distinctive hysteretic nature of polarization against applied voltage, ferroelectric materials have been intensively studied for application to non-volatile random access memory (NvRAM). Ferroelectric $SrBi_2Ta_2O_9$ (SBT), one of the bismuth layer-structured ferroelectrics (BLSFs), is received as a leading candidate because of its excellent fatigue endurance in the form of thin films with Pt electrode [1] : subjected to repetitive polarization switching, SBT does not show a decrease in the amount of remanent charge. Recently bismuth titanate system in the family of BLSF was reported to show fatigue-free properties with relatively large remanent polarization [2]. The fatigue-free nature of BLSFs is considered to originate from their layered structure [1].

BLSF consists of the bismuth oxide layers, $(Bi_2O_2)^{2+}$, and pseudo-perovskite blocks and these are alternately stacked along the crystallographic *c*-axis. The pseudo-perovskite blocks have a formula of $(A_{m-1}B_mO_{3m+1})^{2-}$, where A is mono-, di- or trivalent ions such as Ba^{2+}, Sr^{2+} and Bi^{3+}; B is tetra-, penta- or hexavalent ions such as Ti^{4+} and Ta^{5+}; and *m* is the number of BO_6 octahedra in the pseudo -perovskite blocks (*m*=1, 2, 3, 4 and 5). The crystal structure of Bismuth titanate, $Bi_4Ti_3O_{12}$ (BIT) is shown in Fig. 1 (a). The pseudo-perovskite blocks, $(Bi_2Ti_3O_{10})^{2-}$, of BIT

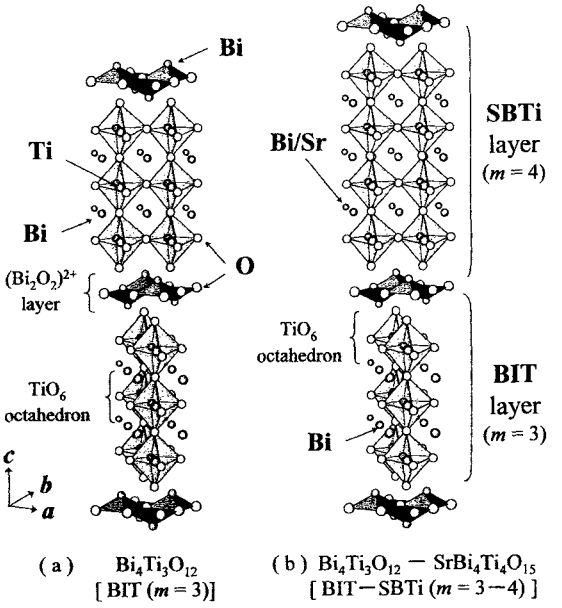

Fig. 1 Schematic representations of the crystal structures for (a) $Bi_4Ti_3O_{12}$ and (b) intergrowth $Bi_4Ti_3O_{12}-SrBi_4Ti_4O_{15}$.

composed of triple TiO_6 octahedral units (m=3) are interleaved with $(Bi_2O_2)^{2+}$ layer, and all of the A site is occupied by Bi^{3+}. The ferroelectricity of BLSFs is attributed to the displacement along the a-axis not only of B-site ions in oxygen octahedra but also of A-site ions [3]. On the other hand, it is widely accepted that the $(Bi_2O_2)^{2+}$ layer plays an important role in preventing fatigue failure[1] : the $(Bi_2O_2)^{2+}$ layers have net electrical charge, and their positioning in the lattice is self-regulated to compensate for space charge near electrodes. For their feasible layered structure, the ferroelectric thin film capacitor with fatigue-free up to 10^{12} polarization switching cycles would be achieved [1]. Up to now, numerous efforts have been focused on the application of the thin films of BLSFs to NvRAM: processing and phase formation of the thin films [4-6], low temperature deposition [7, 8], improvement of leakage and ferroelectric properties [9-12], and crystal orientation [13, 14] *etc.*. Recently, ferroelectric hysteresis of SBT memory cells with lateral size of submicro-meter order has been verified [15], and the study of the practical use of ferroelectric thin films has been progressing markedly. However the understanding of the fundamental physics of BLSFs is far from complete.

A family of intergrowth BLSF [16] is one of the suitable materials for the fundamental study of the relationship between crystal structures and ferroelectric properties. Figure 1 (b) shows the crystal structure of regular intergrowth compound, $Bi_4Ti_3O_{12}-SrBi_4Ti_4O_{15}$ (BIT-SBTi). The pseudo-perovskite block, $(SrBi_2Ti_4O_{13})^{2-}$, of SBTi is composed of four units of TiO_6 octahedra, *i.e.* m=4, and the A site ions comprise Bi^{3+} and Sr^{3+}. The pseudo-perovskite layers, $(Bi_2Ti_3O_{10})^{2-}$ and $(SrBi_2Ti_4O_{13})^{2-}$, with different number of m are alternately stacked in the lattice as shown. The intergrowth structure has been confirmed only in nanoscopic area by a Transmission Electron Microscope [17]. However, it is not clear whether the phase of the intergrowth BLSF is thermodynamically stable and the continuity of intergrowth structure is held all over the crystals or not. Furthermore, there is no detailed report on dielectric properties and the phase transition of intergrowth compounds.

In this paper, the intergrowth BIT-SBTi whose pseudo-perovskite blocks are composed only of TiO_6 octahedra is chosen for the facility of the synthesis and the simple chemical composition. We first report on the evidence of regular intergrowth structure of BIT-SBTi obtained by the Rietveld method, and the ferroelectric phase transition of the BIT-SBTi is shown to be of the first-order type.

2. EXPERIMENTAL PROCEDURE

The ceramic samples of BIT, SBTi and intergrowth BIT-SBTi were prepared by the standard solid-state reaction technique. The powders of $SrCO_3$, Bi_2O_3 and Ta_2O_5 with the purity of 99.99 % were mixed in a ball mill in 12 h. The excess Bi of 3% for BIT, 2% for SBTi, and 1.5% for BIT-SBTi was added to compensate Bi vaporization during the sintering process. The mixed powder calcined at 800 °C for 7 h was crushed and pressed into pellet. Then the pellets were sintered at 830 °C (BIT) and 1200 °C (SBTi and BIT-SBTi) for 1 h. The density of the sample obtained was over 90 % of the theoretical density. For X-ray diffraction (XRD) measurements, the pellets were fired at 800 °C (BIT) and 1100 °C (SBTi and BIT-SBTi) for 12 h to prevent from grain growth and preferred orientation, and then crushed. The powder XRD patterns were obtained by the $2\theta/\theta$ step-scan method from 5° to 80° (2θ) using the step of 0.02° (2θ). The XRD patterns of BIT-SBTi were analyzed by the Rietveld method (the RIETAN program [18]) using the space group of $P2_1am$. The dielectric measurements were performed using the dense samples with about 0.15 mm in thickness. Pt was sputtered on the surface as electrodes.

3. RESULTS AND DISCUSSION

Figure 2 shows the results of the Rietveld analysis

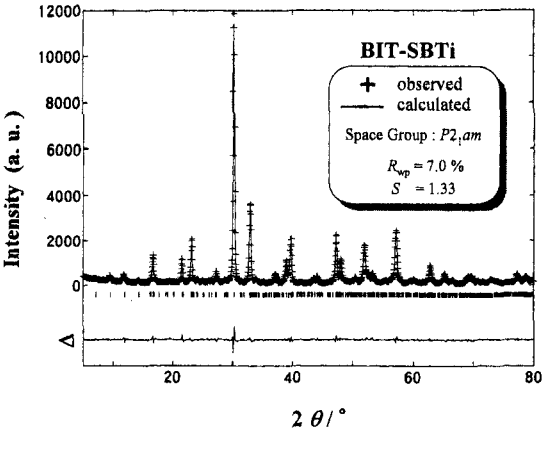

Fig. 2 Result of the Rietveld analysis for the powder XRD pattern of intergrowth BIT-SBTi. The Δ indicates the difference of the observed data (+) and the calculated (−) pattern.

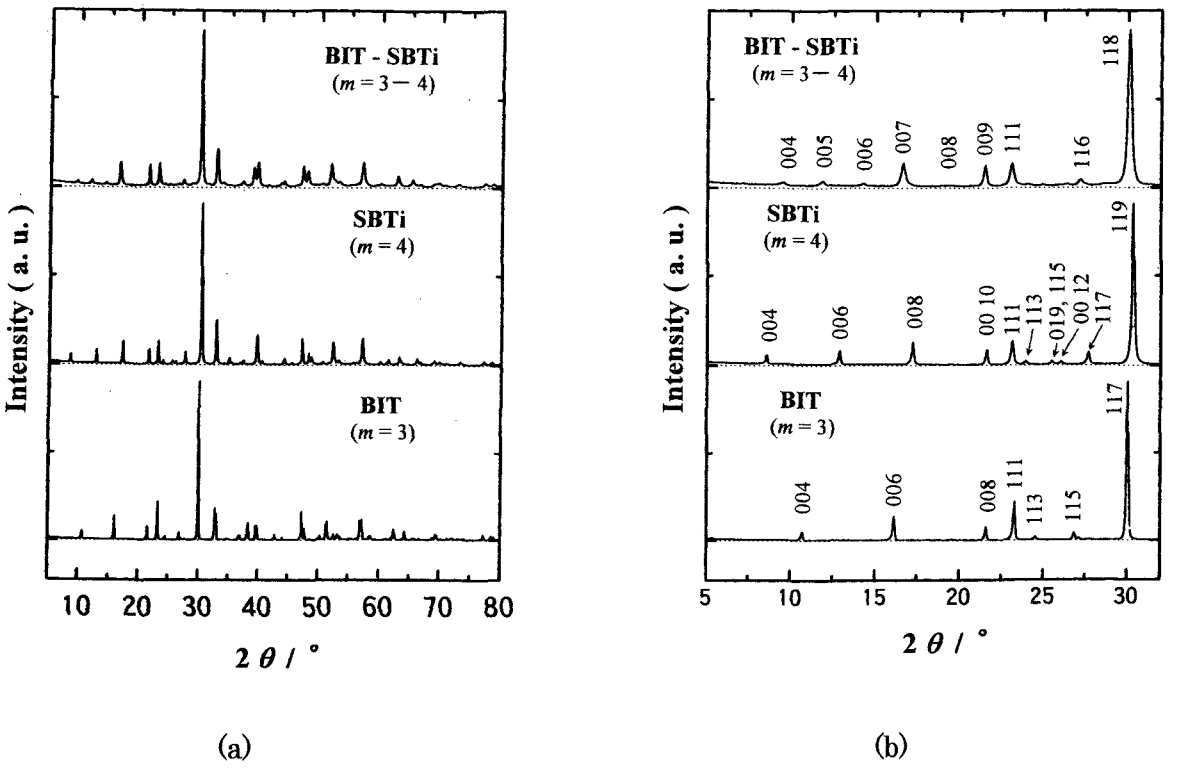

Fig.3 Comparison of powder XRD patterns of BIT, SBTi and intergrowth BIT-SBTi. Figure (b) is the expansion of the low 2θ angle part.

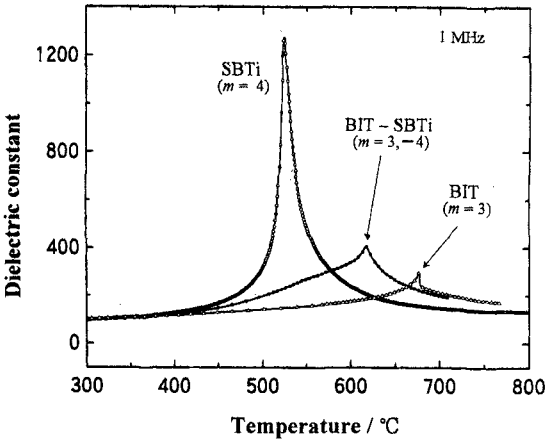

Fig. 3 Temperature dependence of dielectric constant.

for intergrowth BIT-SBTi. The calculated pattern fits fairly well to the observed data and the *R*-weighted pattern, R_{wp}, and Goodness of fit, *S*, which are standards of the degree of difference of those, are very small. These results demonstrate that the regular intergrowth structure of the order of nanometer scale as shown in Fig. 1(b) spreads through the crystal and the single phase of the intergrowth BIT-SBTi was obtained.

The lattice constants estimated by the Rietveld analysis are summarized in Table 1. While the *b* and the *c* of BIT-SBTi became the average of those for BIT

Table 1 Lattice constants

	a / nm	*b* / nm	*c* / nm
BIT (*m* = 3)	0.54472(33)	0.54086(33)	3.2819(21)
SBTi (*m* = 4)	0.5453(12)	0.5467(12)	4.1098(85)
BIT-SBTi (*m*=3-4)	0.54257(98)	0.54455(99)	3.6923(67)

and SBTi, the *a* was shortest. The ferroelectricity of BLSFs mainly originates from the displacement of A- and B-site ions along the *a*-axis, and the lattice constant *a* is strongly related to the ferroelectric properties. The shorter *a* of BIT-SBTi could be attributed to the strong ferroelectric interaction between two kinds of perovskite blocks in the intergrowth structure.

The comparison of the XRD patterns between the intergrowth BIT-SBTi and the constituent BLSFs are depicted in Fig. 3. Above 2θ of 20 ° , the patterns of three compounds are nearly the same, especially there is no difference between the peaks of intergrowth BIT-SBTi and BIT practically. These results suggest that it is difficult to identify phases of BLSFs from a simple assignment of the XRD peaks and a misunderstanding phase could be deduced for the worst. The difference among them can be seen only in the XRD

patterns at very low angle below 2θ of 20 ° as shown in Fig. 3(b). While for BIT and SBTi, normal BLSFs, the peaks of 00*l* with even number of *l* are observed because of the regular period of the Bi_2O_2 layer in the lattice, the intergrowth compounds have the 00*l* peaks not only with even number of *l* but also with odd number of *l*, which is a distinguishing feature of intergrowth compounds. These results of XRD patterns are quite reasonable from the viewpoint of their crystal structure. As mentioned in INTRODUCTION, these three compounds consist of Bi_2O_2 layers and pseudo-perovskite blocks, and their structure in *a-b* plane is almost the same. The structural differences of those are the number of BO_6 octahedra, *i.e.*, the length between the Bi_2O_2 layers and the stacking of Bi_2O_2 layers and pseudo-perovskite blocks along the *c*-axis, being reflected in the peaks of 00*l* at low angle of 2θ.

The temperature dependences of dielectric constant are shown in Fig. 4. While the Curie temperature, T_c, of BIT and SBTi is 675 °C and 520 °C, respectively, the peak of dielectric constant for their intergrowth compounds appeared at almost the middle of those, around 610 °C. For the further investigation of ferroelectric phase transition, differential thermal analysis (DTA) measurement was carried out using broken pieces of the samples. For BIT, sharp endo- and exothermic peaks were observed, which shows that the ferroelectric phase transition of BIT is of the first-order type. On the other hand, any peak was not detected for SBTi. In the case of intergrowth BIT-SBTi, the DTA signal caused by both endo- and exothermic structural change appeared around the peak of the dielectric constant. This DTA result of the intergrowth BIT-SBTi is the direct evidence for the ferroelectric phase transition of the first-order type . The ferroelectric phase transition at the middle of the T_c of the constituent BIT and SBTi suggests a strong interaction between two kinds of perovskite layers arcos Bi_2O_2 layers. Further investigation of dielectric dissipation and ferroelectric properties such as remanent polarization and coercive electric field will be reported elsewhere.

4. CONCLUSIONS

A Rietveld analysis of the intergrowth BIT-SBTi was performed and the continuity of the regular intergrowth structure was verified to spread through the crystal. Comparing the powder XRD patterns with constituent BIT and SBTi, the difference appeared only at very low 2θ angle and the distinguishing peaks of intergrowth compound were found to be 00*l* with odd number of *l*. The dielectric and DTA measurement reveled that the ferroelectric phase transition of the intergrowth BIT-SBTi occurred at the middle of the Curie temperatures of constituent BIT and SBTi and was of the first-order type.

ACKNOWLEDGEMENT

The authors would like to acknowledge M. Hibino for his helpful discussion about the Rietveld analysis.

REFERENCES

[1] C. A-Paz de Araujo, J. D. Cuchiaro, L. D. Mcmillan, M. C. Scott and J. F. Scott, *Nature* **374**, 627 (1995).

[2] B. H. Park, B. S. Kang, S. D. Bu, T. W. Noh, J. Lee, and W. Joe, *Nature* **401**, 682(1999)

[3] R. L. Withers, J. G. Thompson and A. D. Rae, *J. Solid State Chem.* **94**, 404 (1991).

[4] P. C. Joshi, S. B. Krupanidhi, A. Mansingh, *J. Appl. Phys.* **72**, 5517 (1992).

[5] G. H. Hu, J. B. Xu, I. H. Wilson, W. Y. Cheung, N. Ke. S. P. Wong, *Appl. Phys. Lett.* **74**, 3711 (1999).

[6] S. D. Bu, B. H. Park, B. S. Kung, S. H. Kung and T. W. Noh, W. Jo, *Appl. Phys. Lett.* **75**, 1155 (1999).

[7] S. O. Ryu, P. C. Joshi, S. B. Desu, *Appl. Phys. Lett.* **75**, 2126 (1999).

[8] T. Kijima, M. Ushikubo and H Matsunaga, *Jpn, J. Appl. Phys.* **38**, 127 (1999).

[9] T. Atsuki, N. Soyama, T. Yonezawa, K. Ogi, *Jpn, J. Appl. Phys.* **34**, 5096 (1995).

[10] C. R. Foschini, E. Longo, J. A. Varela, S. B. Desu, *Appl. Phys. Lett.* **75**, 552 (1999).

[11] M. Noda, Y. Matsumuro, H. Sugiyama and M. Okuyama, *Jpn. J. Appl. Phys.* **38**, 2275 (1999).

[12] H.-M. Tsai, P. Lin and T.-Y. Tseng, *J. Appl. Phys.* **85**, 1095 (1999).

[13] N. Fujimura, D. T. Thomas, S. K. Streiffer, A. I. Kingon, *Jpn, J. Appl. Phys.* 37, 5185 (1998).

[14] K. Ishikawa, H. Hunakubo, *Appl. Phys. Lett.* 75, 1970 (1999).

[15] M. Alex, C. Harnagea, D. Hesse and U. Gösele, *Appl. Phys. Lett.* 75, 1793 (1999).

[16] T. Kikuchi, A. Watanabe, and K. Uchida, Mater. Res. Bull. **12**, 299 (1977).

[17] D. A. Jefferson, M. K. Uppal, and C. N. R. Rao, Mater. Res. Bull. **19**, 1403 (1984).

[18] F. Izumi, " *The Rietveld Method*" ed. by R. A. Young, Oxford University Press, Oxford, Chap. 13 (1993).

(Received December 16,1999 ; Accepted January 31,2000)